Non-covalent functionalization of graphene with a hydrophilic self-limiting monolayer for macro-molecule immobilization

Concha Bosch-Navarro [a,b,⇑], Zachary P.L. Laker [a], Alexander J. Marsden [a], Neil R. Wilson [a], Jonathan P. Rourke [b]

[a] Department of Physics, University of Warwick, Coventry CV4 7AL, UK
[b] Department of Chemistry, University of Warwick, Coventry CV4 7AL, UK

a r t i c l e   i n f o

a b s t r a c t

Two different pyrene-substituted ions were used to render the surface of graphene hydrophilic. Self-limiting monolayers of ammonium and sulfonate substituted pyrenes were used to give, respectively, an overall positive and negative charge to the surface. Both pyrenes gave a stable hydrophilic surface and were used to selectively immobilise negatively or positively charged macro-molecules. This simple and versatile non-covalent approach can be used on graphene on a variety of substrates (e.g. copper, SiO_2), suspended graphene, and also for graphite.

Introduction

Graphene displays a remarkable combination of properties: it has high thermal conductivity and high charge carrier mobility, it is almost optically transparent, and is strong, stiff and flexible [1]. This has led to many proposed applications, including in sens-ing [2–4] and catalysis [5,6]. However, its simple and robust struc-ture also leads to some difficulties: like graphite, it is hydrophobic and its smooth van der Waals surface does not lend itself to selec-tive adsorption of biomaterials [7,8]. This makes sensors based on pristine graphene unselective in their response, and leads to com-patibility issues for aqueous processing routes. Hence, for many applications, controlling graphene's surface functionality becomes essential. This necessitates chemical modification which should be done in such a way so as to retain the beneficial physical properties of graphene and in as thin a modified layer as possible so as to maximise the contribution of graphene to the hybrid material. Even low-level covalent functionalisation rapidly degrades the electronic properties of graphene [9–11], so non-covalent func-tionalisation which retains the sp^2 graphene structure is preferred.

Molecules with planar delocalised p systems are often chosen for non-covalent functionalisation of graphene [11], as these can interact with the extended electronic system of the graphene sur-face by van der Waals or electrostatic interactions, commonly referred to as p stacking [12]. To this end, layers of small molecules on graphene such as perylenebisimides [13–15], phthalocyanines [16,17] or pyrenes (pyr) [18–22] have been investigated. Pyr derivatives are particularly interesting as their chemical versatility has been widely exploited to create carbon-based hybrid materials through p stacking [23–27], and to assist the exfoliation of graphite to graphene [28–31]. Hence, they provide an easy and flexible route to modifying the surface properties of graphene. Here we design pyrene derivatives to form self-limiting monolayer films on graphene in order to make the surface positively or negatively charged in solution. This turns the graphene from hydrophobic to hydrophilic and enables controlled macro-molecule adsorption through electrostatic interactions.

Results and discussion

We designed pyrene derivatives that would non-covalently bind to the Gr surface, but would remain non-reactive. Thus, we attached non-coordinating charged moieties via a flexible linker to a pyrene core, as shown in Fig. 1. The pyr-carrying ammonium cation (trimethyl-(2-oxo-2-pyren-1-yl-ethyl)-ammonium bro-mide; pyr^+) [32] and pyr-carrying sulfonate anion (sodium (2-oxo-2-pyren-1-yl-ethyl)-sulfonate; pyr) were synthesized (for details see SI1). During deposition from solution, the hydrophobic p-conjugated pyrene core should bind strongly to the Gr surface by p stacking, whilst electrostatic repulsion between the charged moieties should self-limit the film to monolayer coverage.

⇑ Corresponding author.
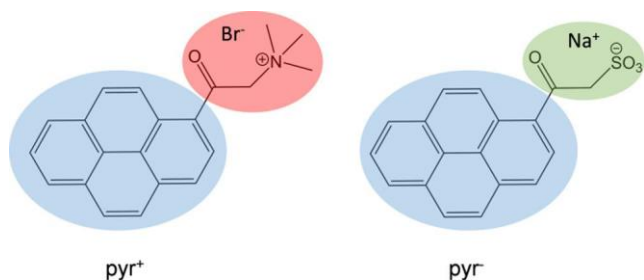 E-mail address: concepcion.bosch@uv.es (C. Bosch-Navarro).

Fig. 1. Representation of trimethyl-(2-oxo-2-pyren-1-yl-ethyl)-ammonium bro-mide (pyr$^+$) and sodium (2-oxo-2-pyren-1-yl-ethyl)-sulfonate) (pyr). The mole-cules consist of a hydrophopic part (highlighted in blue) designed to adhere to the surface of graphene through p-p forces, and a charged moiety (highlighted in red and green) that then controls the surface functionality.

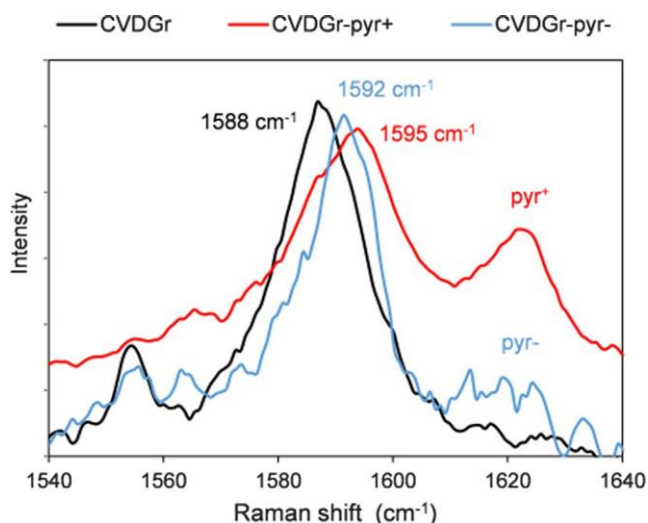
Fig. 2. Raman spectra of CVDGr (black), CVDGr-pyr$^+$ (red) and CVDGr-pyr (blue). The spectra were acquired with an excitation line of 633 nm.

To test this, the pyr-derivatives were deposited on chemical vapour deposition (CVD) grown graphene on copper. This is an ideal substrate for studying molecular deposition on graphene [13,17]: it is of technological relevance and presents a clean, flat and well defined surface for detailed studies. Large area monolayer graphene was synthesized by CVD on copper foil using methane as the precursor (for details see methods and Supplementary Infor-

mation Section 1, SI1) and its uniformity and quality were con-firmed by scanning electron microscopy and Raman spectroscopy (SI2-SI3). As-produced graphene-on-copper (CVDGr) samples were immersed overnight in ethanolic solutions containing the pyr$^+$ molecule, or methanolic solutions containing the pyr molecule. After drying, Raman spectroscopy confirmed the presence of the pyrene derivatives on the CVDGr, with a new band corresponding to the pyr moieties appearing at around 1620 cm^{-1} as shown in Fig. 2 (see also SI3). Moreover, the graphene G band upshifts by 4–7 cm^{-1} (from 1588 cm^{-1} in CVDGr to 1592 cm^{-1} in CVDGr-pyr$^+$ and to 1595 cm^{-1} in CVDGr-pyr), indicative of electrostatic doping of Gr by the charged moieties after functionalization [20,33–35]. X-ray photoelectron spectroscopy (XPS) further con-firmed the presence of pyr$^+$ and pyr , and proved that only a very thin layer of modified pyr was deposited on the CVDGr, consistent with a monolayer coverage (see SI4). Atomic force microscopy (AFM) analysis showed that the deposited layers of pyr$^+$ and pyr on CVDGr were thin and homogeneous. Topography images (Fig. 3a and SI6 for CVDGr-pyr$^+$ and CVDGr-pyr , respectively) after surface modification are almost indistinguishable from CVDGr, showing the facets that form on the copper substrate after gra-phene growth [36] and with no obvious pyr agglomerates. The presence of the pyr$^+$/pyr films is revealed by selectively removing small regions by first scanning in contact mode (controllably scratching away the molecular layer) and then scanning a larger region in tapping mode and hence scanning across covered and uncovered areas (Fig. 3b). AFM height profiles (Fig. 3c and SI6) indicate the presence of a thin molecular layer on the Gr of about 0.2 nm for both CVDGr-pyr$^+$ and CVDGr-pyr , observable due to the locally smooth graphene on copper surface [37], again consis-tent with monolayer coverage. We note that by contrast similar depositions of unmodified pyrene on CVDGr appeared to form three dimensional islands rather than uniform monolayers (SI7). Scanning tunnelling microscopy (STM) investigations under ambi-ent conditions were unfortunately unable to resolve the molecular packing. Ab initio calculations have shown that pyr stably adsorbs flat to graphene, and that the binding energy increases when elec-tron donating or withdrawing groups are substituted to the pyr [38]. Hence, although previous reports have found that pyrene can desorb in solution [21], with electropolymerisation a possible approach to stabilising them [22], here we found the modified pyr-ene layers to be stable. However, at room temperature the pyr are expected to move rapidly along the graphene surface and hence would not be easily visible by STM.

Static contact angle measurements (SCA) were performed to examine the wetting properties of CVDGr before and after non-
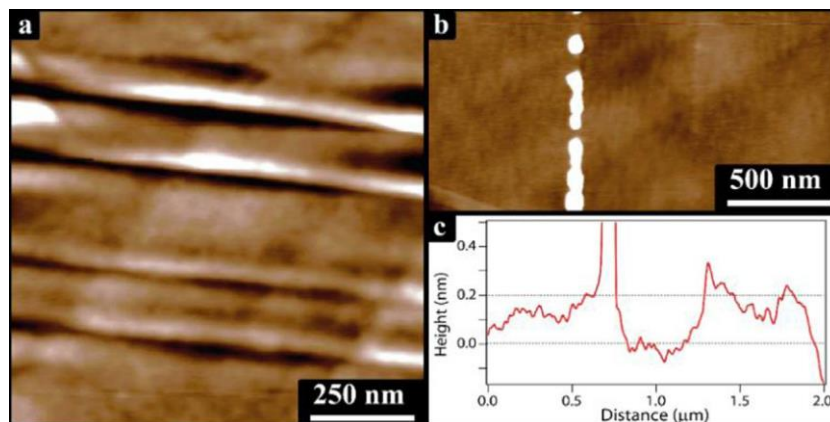

Fig. 3. a) AFM topography image of CVDGr-pyr$^+$. b) AFM topography image showing the scratch over CVDGr-pyr$^+$ created by employing AFM in contact mode, root mean square roughness excluding the scratch is 0.3 nm. c) Height profile corresponding to (b), consistent with the presence of a monolayer of pyr$^+$ over CVDGr. The full height scales of the AFM images are 5 nm.
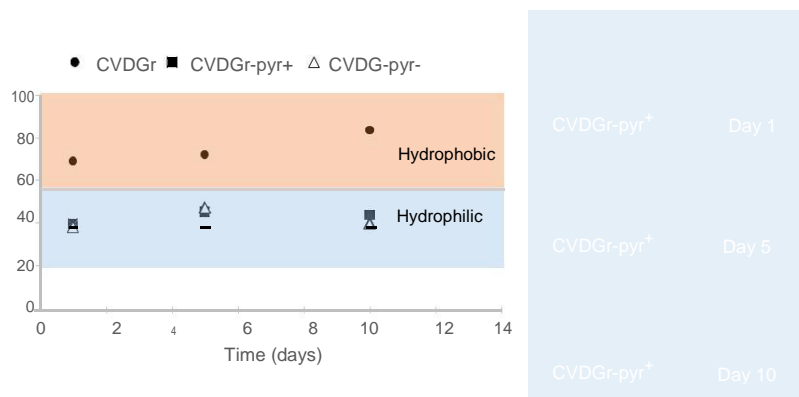
Fig. 4. Left: Time dependency of the static contact angle for water on CVDGr (circles), CVDGr-pyr$^+$ (squares) and CVDGr-pyr (triangles). Right: Photographs of contact angle measurements acquired for CVDGr-pyr$^+$ after 1, 5 and 10 days storage under ambient conditions.
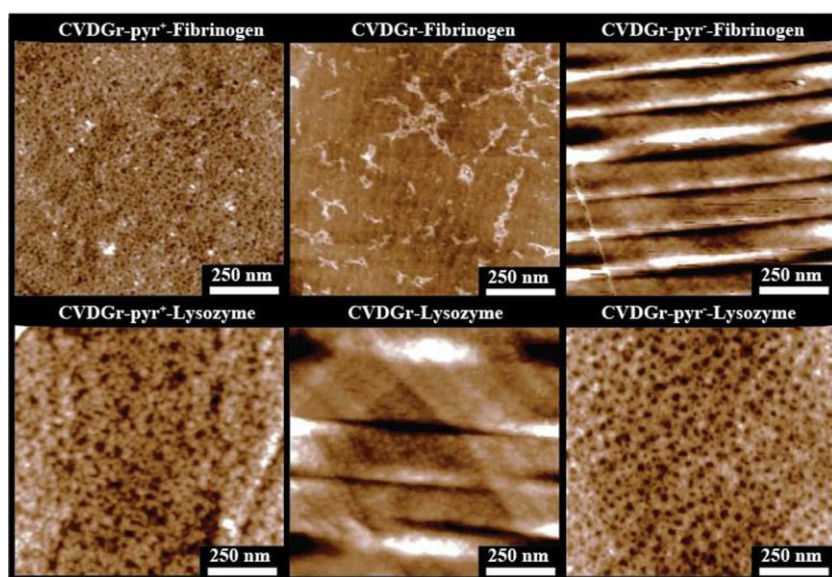

Fig. 5. AFM topographic images of CVDGr-pyr$^+$ (left), CVDGr (middle) and CVDGr-pyr (right) after incubation with fibrinogen (top row) and lysozyme (bottom row). The full height scale of the AFM images is 5 nm.

covalent functionalisation with the pyr$^+$/pyr . As-produced CVDGr was found to be hydrophobic, with contact angles initially around 70L but increasing to 82L when measured 10 days after growth, Fig. 4, consistent with previous reports [39–42]. After deposition of pyr$^+$/pyr , the contact angle dropped to ca. 40L demonstrating that the surface was now hydrophilic. This result was reproducible and consistent for both CVDGr-pyr$^+$ and CVDGr-pyr samples, with a uniform response across samples suggesting a homogeneous deposition of the pyr molecules (SI5). In addition, for both CVDGr-pyr$^+$ and CVDGr-pyr the contact angle remained almost constant (SCA 40L) at least for one month, demonstrating that the adsorbed molecular layers provide a simple, robust and stable method for changing the surface properties of graphene.

Many macro-molecules are charged in solution [43], hence elec-trostatic interactions can be a powerful way of controlling their adhesion. To test this, we studied the adsorption of biomolecules onto the graphene surface with and without modification.

Initially we looked at biomolecule adsorption on the graphene on copper surface by studying an anionic (negatively charged) pro-tein (fibrinogen) as well as lysozyme, a protein which, at pH 7, con-tains regions of both positive and negative charge [43]. These molecules are of interest in their own right: fibrinogen is about

46 nm in length and 50–70 Å in diameter, is essential to the forma-tion of blood clots and is often employed as a model protein to evaluate the biocompatibility of surfaces [44] whilst lysozyme is a bacteriolytic enzyme consisting of a single polypeptide chain of about 129 aminoacids [45].

To test the interactions between the (un)modified graphene surface and the biomolecules, CVDGr was incubated for 3 min in a phosphate buffer solution (pH 7) containing either fibrinogen or lysozyme (2 lg/mL), dried and then analysed by AFM. For the unmodified graphene, a sparse distribution of biomolecules is observed (see Fig. 5) indicating a low affinity for both of the biomo-lecules, consistent with previous reports [44]. The pyr$^+$ modified graphene showed a strong affinity for the negatively charged fib-rinogen which formed a near continuous layer (Fig. 5). By contrast, no fibrinogen is observed on pyr modified graphene. Consistent with its ambipolar nature, lysozyme forms near continuous layers on both pyr$^+$ and pyr modified graphene (Fig. 5). To ensure that this was not just a drying artefact, samples were also analysed by AFM imaging in liquid during the deposition (SI8) and showed results consistent with the dry samples. The charged pyrene derivatives are thus effective at controlling biomolecule adsorption on graphene surfaces.
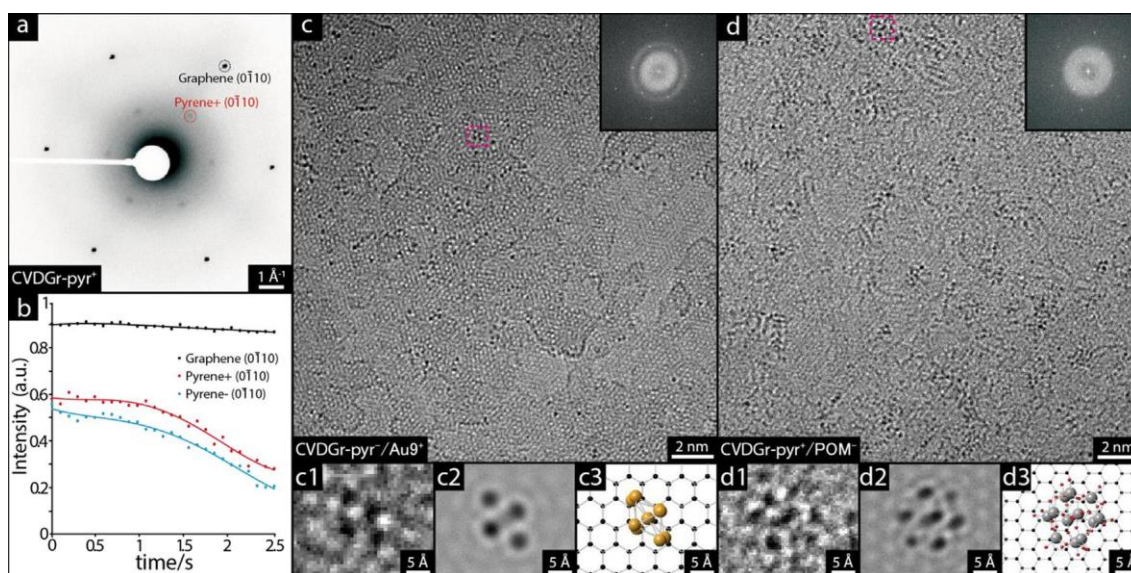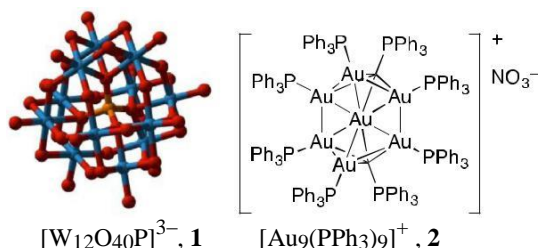
Fig. 6. a) TEM low-dose diffraction of CVDGr-pyr$^+$ b) Diffraction spot intensities plotted as a function of time for graphene at a dose rate of 4 e Å^2 s^1 for CVDGr-pyr$^+$ and CVDGr-pyr demonstrating their beam-sensitive nature. c) and d) are acTEM images showing Au9 clusters attached to CVDGr-pyr and POM clusters attached to CVDGr-pyr$^+$ respectively, with inset FFT showing the characteristic hexagonal pattern of graphene monolayer. A magnified view of the boxed areas, c1 and d1, are shown alongside corresponding multi-slice simulations, c2 and d2, and atomic models, c3 and d3.

To illustrate the versatility of this approach, we tested deposi-tion of the pyr-derivatives on graphene transferred to a SiO$_2$ sub-strate, and also on highly oriented pyrolytic graphite. On both substrates the pyr-derivatives formed thin films consistent with those on CVDGr, and on both substrates they enabled controlled adhesion of biomolecules (see AFM images in SI9).

Finally, the potential for controlling macromolecule adsorption on suspended graphene membranes was assessed. Graphene mem-branes have proven to be useful supports for a variety of micro-scopies, particularly electron microscopy [18,32–39]. However, functionalisation is required to uniformly deposit the material to be studied [18]. To test the efficacy of the modified pyrenes for this application, two oppositely charged inorganic clusters of defined atomic structure were chosen. Each is readily identified by trans-mission electron microscopy (TEM): the anionic polyoxometalate (POM) phosphotungstic acid ([W$_{12}$O$_{40}$P]$^{3-}$, 1) and the cationic nan-ocluster [Au$_9$(PPh$_3$)$_9$]$^+$ (2, abbreviated henceforth as Au9) [32–34]. Both have been studied by TEM before [46,47], both are of interest in their own right for applications such as catalysis, but most importantly here, both can be positively identified by aberration-corrected TEM (acTEM) due to their distinctive atomic geometries (see Fig. 6 and SI10/SI11).

[W$_{12}$O$_{40}$P]$^{3-}$, **1**   [Au$_9$(PPh$_3$)$_9$]$^+$, **2**

Suspended graphene membranes were fabricated by transferral of CVDGr to TEM grids (see Methods) and functionalised by immer-sion overnight in solutions of pyr$^\pm$. As shown in Fig. 6a), diffraction analysis of the pyr modified graphene membranes showed the characteristic hexagonal diffraction pattern of graphene, but also

an inner hexagon of diffraction spots, aligned to those of graphene, corresponding to a lattice parameter of 0.28 ± 0.01 nm, similar to previously reported for a pyrene derivative on graphene[28]. These inner spots decayed rapidly with exposure to the electron beam, Fig. 6b), with a critical dose of 10 e Å^2, as to be expected for a molecular overlayer with only weak, non-covalent, intermolecular bonds. The diffraction thus shows the presence of the pyrene and indicates that it is forming an ordered layer. The low critical dose unfortunately precluded direct imaging of the molecular layer by acTEM.

Atomic resolution acTEM verified the selective adsorption of anionic clusters on pyr+, and cationic on pyr-, modified graphene. The pyr$^\pm$-graphene TEM grids were incubated for 3 min in a solu-tion containing either the POM (0.1 mg/mL) or Au9 (1 mg/mL), dried and then analysed by acTEM. Note that the pyr molecular layers are destroyed by the electron beam dose required for high resolution imaging (here typically > 100 e Å^2) and so are not apparent in these images. The pyr$^+$ modified graphene showed a strong affinity for the negatively charged POM with average cover-age measured to be 500 ± 10 molecules ɪm^2, identified by their signature atomic arrangement (Fig. 6d). By contrast, no POM is observed on pyr or un-modified graphene (SI12). Consistent with its cationic nature, the pyr modified graphene showed a strong affinity for the

Au9 with average coverage measured to be 100 ± 10 molecules ɪm^2 (Fig. 6c). By contrast, no Au9 is observed on pyr$^+$- or un-modified graphene (SI12). Coupling together the AFM and acTEM studies, this clearly demonstrates how control over the electro-static interactions enables control over the adsorption of a variety of macro-molecules. As a result we expect these pyr-derivatives to be widely effective for surface modification of graphene based materials.

Conclusions

In conclusion, we have shown how the surface functionality of graphene can be easily tuned with self-limiting monolayer films of pyr-modified ions. These enable control over electrostatic inter-actions in solution to selectively bind charged macro-molecules, and similarly should be effective for other charged species. We

expect this approach to be generically applicable to graphene on any surface or indeed free-standing, making it useful in a wide variety of fields including biomedicine, electrochemical sensors or catalysis, as well as for selective adsorption to supported gra-phene membranes for cryo- and acTEM imaging.

Acknowledgement

References

[1] A.C. Ferrari, Science and technology roadmap for graphene, related two-dimensional crystals, and hybrid systems, Nanoscale (2014).

[2] J.G. Martínez, T.F. Otero, H. Prima-Garcia, C. Martí-Gastaldo, C. Bosch-Navarro, E. Coronado, Graphene electrochemical responses sense surroundings, Electrochim. Acta 81 (2012) 49–57.

[3] S.S. Varghese, S. Lonkar, K.K. Singh, S. Swaminathan, A. Abdala, Recent advances in graphene based gas sensors, Sens. Actuators B Chem. 218 (2015) 160–183.

[4] P.A. Pandey, N.R. Wilson, J.A. Covington, Pd-Doped reduced graphene oxide sensing films for H2 detection, Sens. Actuators B Chem. 183 (2013) 478–487.

[5] G. Xie, K. Zhang, B. Guo, Q. Liu, L. Fang, J.R. Gong, Graphene-based materials for hydrogen generation from light-driven water splitting, Adv. Mater. 25 (2013) 3820–3839.

[6] B.F. Machado, P. Serp, Graphene-based materials for catalysis, Catal. Sci. Technol. 2 (2012) 54–75.

[7] O. Leenaerts, B. Partoens, F. Peeters, Water on graphene: hydrophobicity and dipole moment using density functional theory, Phys. Rev. B 79 (2009) 235440.

[8] S. Wang, Y. Zhang, N. Abidi, L. Cabrales, Wettability and surface free energy of graphene films, Langmuir 25 (2009) 11078–11081.

[9] A.J. Marsden, P. Brommer, J.J. Mudd, M.A. Dyson, R. Cook, M. Asensio, J. Avila, A. Levy, J. Sloan, D. Quigley, et al., Effect of oxygen and nitrogen functionalization on the physical and electronic structure of graphene, Nano Res. 8 (2015) 2620–2635.

[10] V. Georgakilas, J.N. Tiwari, K.C. Kemp, J.A. Perman, A.B. Bourlinos, K.S. Kim, R. Zboril, Noncovalent functionalization of graphene and graphene oxide for energy materials, biosensing, catalytic, and biomedical applications, Chem. Rev. 116 (2016) 5464–5519.

[11] V. Georgakilas, M. Otyepka, A.B. Bourlinos, V. Chandra, N. Kim, K.C. Kemp, P. Hobza, R. Zboril, K.S. Kim, Functionalization of graphene: covalent and non-covalent approaches, derivatives and applications, Chem. Rev. 112 (2012) 6156–6214.

[12] C.R. Martinez, B.L. Iverson, Rethinking the term 'Pi-Stacking', Chem. Sci. 3 (2012) 2191–2201.

[13] N.C. Berner, S. Winters, C. Backes, C. Yim, K.C. Dümbgen, I. Kaminska, S. Mackowski, A.A. Cafolla, A. Hirsch, G.S. Duesberg, Understanding and optimising the packing density of perylene bisimide layers on CVD-grown graphene, Nanoscale 7 (2015) 16337–16342.

[14] S. Winters, N.C. Berner, R. Mishra, K.C. Dümbgen, C. Backes, M. Hegner, A. Hirsch, G.S. Duesberg, On-surface derivatisation of aromatic molecules on graphene: the importance of packing density, Chem. Commun. 51 (2015) 16778–16781.

[15] A. Hirsch, J.M. Englert, F. Hauke, Wet chemical functionalization of graphene, Acc. Chem. Res. 46 (2013) 87–96.

[16] P.A. Pandey, L.A. Rochford, D.S. Keeble, J.P. Rourke, T.S. Jones, R. Beanland, N.R. Wilson, Resolving the nanoscale morphology and crystallographic structure of molecular thin films: F16CuPc on graphene oxide, Chem. Mater. 1365–1370 (2012).

[17] A.J. Marsden, L.A. Rochford, D. Wood, A.J. Ramadan, Z.P.L. Laker, T.S. Jones, N.R. Wilson, Growth of Large Crystalline Grains of Vanadyl-Phthalocyanine Without Epitaxy on Graphene, Adv. Funct. Mater. (2016).

[18] G.F. Schneider, Q. Xu, S. Hage, S. Luik, J.N.H. Spoor, S. Malladi, H. Zandbergen, C. Dekker, Tailoring the hydrophobicity of graphene for its use as nanopores for DNA translocation, Nat. Commun. 4 (2013) 1–7.

[19] S. Ghosh, X. An, R. Shah, D. Rawat, B. Dave, S. Kar, S. Talapatra, Effect of 1-pyrene carboxylic-acid functionalization of graphene on its capacitive energy storage, J. Phys. Chem. C 116 (2012) 20688–20693.

[20] R.S. Pantelic, W. Fu, C. Schoenenberger, H. Stahlberg, Rendering graphene supports hydrophilic with non-covalent aromatic functionalization for transmission electron microscopy, Appl. Phys. Lett. 104 (2014) 134103.

[21] J.A. Mann, J. Rodríguez-López, H.D. Abruña, W.R. Dichtel, Multivalent binding motifs for the noncovalent functionalization of graphene, J. Am. Chem. Soc. 133 (2011) 17614–17617.

[22] M. Singh, M. Holzinger, M. Tabrizian, S. Winters, N.C. Berner, S. Cosnier, G.S. Duesberg, Noncovalently functionalized monolayer graphene for sensitivity enhancement of surface plasmon resonance immunosensors, J. Am. Chem. Soc. 137 (2015) 2800–2803.

[23] G. Katsukis, J. Malig, C. Schulz-Drost, S. Leubner, N. Jux, D.M. Guldi, Toward combining graphene and QDs: assembling CdTe QDs to exfoliated graphite and nanographene in water, ACS Nano 6 (2012) 1915–1924.

[24] C. Ehli, G.M.A. Rahman, N. Jux, D. Balbinot, D.M. Guldi, F. Paolucci, M. Marcaccio, D. Paolucci, M. Melle-Franco, F. Zerbetto, et al., Interactions in single wall carbon nanotubes/pyrene/porphyrin nanohybrids, J. Am. Chem. Soc. 128 (2006) 11222–11231.

[25] C.-L. Chung, C. Gautier, S. Campidelli, A. Filoramo, Hierarchical functionalisation of single-wall carbon nanotubes with DNA through positively charged pyrene, Chem. Commun. 46 (2010) 6539–6541.

[26] C. Bosch-Navarro, B. Matt, G. Izzet, C. Romero-Nieto, K. Dirian, A. Raya, S.I. Molina, A. Proust, D.M. Guldi, C. Martí-Gastaldo, et al., Charge transfer interactions in self-assembled single walled carbon nanotubes/dawson–wells polyoxometalate hybrids, Chem. Sci. 5 (2014) 4346–4354.

[27] J. Malig, C. Romero-Nieto, N. Jux, D.M. Guldi, Integrating water-soluble graphene into porphyrin nanohybrids, Adv. Mater. 24 (2012) 800–805.

[28] A. Schlierf, H. Yang, E. Gebremedhn, E. Treossi, L. Ortolani, L. Chen, A. Minoia, V. Morandi, P. Samorì, C. Casiraghi, et al., Nanoscale insight into the exfoliation mechanism of graphene with organic dyes: effect of charge, dipole and molecular structure, Nanoscale 5 (2013) 4205.

[29] Y. Xu, B. Hua, G. Lu, Flexible graphene films via the filtration of water-soluble noncovalent functionalized graphene sheets, J. Am. Chem. Soc. 130 (2008) 5856–5857.

[30] X. An, T. Simmons, R. Shah, C. Wolfe, K.M. Lewis, M. Washington, S.K. Nayak, S. Talapatra, S. Kar, Stable aqueous dispersions of noncovalently functionalized graphene from graphite and their multifunctional high-performance applications, Nano Lett. 10 (2010) 4295–4301.

[31] X. Dong, Y. Shi, Y. Zhao, D. Chen, J. Ye, J. Yao, F. Gao, Z. Ni, T. Yu, Z. Shen, et al., Symmetry breaking of graphene monolayers by molecular decoration, Phys. Rev. Lett. 102 (2009) 135501.

[32] N. Nakashima, Ã.Y. Tomonari, H. Murakami, Water-soluble single-walled carbon nanotubes via noncovalent sidewall-functionalization with a pyrene-carrying ammonium ion, Chem. Lett. 638–639 (2002).

[33] X. Dong, D. Fu, W. Fang, Y. Shi, P. Chen, L.-J. Li, Doping single-layer graphene with aromatic molecules, Small 5 (2009) 1422–1426.

[34] A. Das, S. Pisana, B. Chakraborty, S. Piscanec, S.K. Saha, U.V. Waghmare, K.S. Novoselov, H.R. Krishnamurthy, A.K. Geim, A.C. Ferrari, et al., Monitoring dopants by raman scattering in an electrochemically top-gated graphene transistor, Nat. Nanotechnol. 3 (2008) 210–215.

[35] J.H. Bong, O. Sul, A. Yoon, S.-Y. Choi, B.J. Cho, Facile graphene n-doping by wet chemical treatment for electronic applications, Nanoscale 6 (2014) 8503–8508.

[36] N.R. Wilson, A.J. Marsden, M. Saghir, C.J. Bromley, R. Schaub, G. Costantini, T.W. White, C. Partridge, A. Barinov, P. Dudin, et al., Weak mismatch epitaxy and structural feedback in graphene growth on copper foil, Nano Res. 6 (2013) 99–112.

[37] A.J. Marsden, M. Phillips, N.R. Wilson, Friction force microscopy: a simple technique for identifying graphene on rough substrates and mapping the orientation of graphene grains on copper, Nanotechnology 24 (2013) 255704.

[38] S. Bailey, D. Visontai, C.J. Lambert, M.R. Bryce, H. Frampton, D. Chappell, A study of planar anchor groups for graphene-based single-molecule electronics, J. Chem. Phys. 140 (2014) 54708.

[39] J. Rafiee, X. Mi, H. Gullapalli, A.V. Thomas, F. Yavari, Y. Shi, P.M. Ajayan, N.A. Koratkar, Wetting transparency of graphene, Nat. Mater. 11 (2012) 217–222.

[40] R. Raj, S.C. Maroo, E.N. Wang, Wettability of graphene, Nano Lett. 13 (2013) 1509–1515.

[41] C.-Y. Lai, T.-C. Tang, C.A. Amadei, A.J. Marsden, A. Verdaguer, N. Wilson, M. Chiesa, A Nanoscopic approach to studying evolution in graphene wettability, Carbon 80 (2014) 784–792.

[42] Z. Li, Y. Wang, A. Kozbial, G. Shenoy, F. Zhou, R. McGinley, P. Ireland, B. Morganstein, A. Kunkel, S.P. Surwade, et al., Effect of airborne contaminants on the wettability of supported graphene and graphite, Nat. Mater. 12 (2013) 925–931.

[43] P.G. Riguetti, T. Caravaggio, Isoelectric points and molecular weights of proteins, J. Chromatogr. 127 (1976) 1–28.

[44] L.E. Averett, M.H. Schoenfisch, Atomic force microscope studies of fibrinogen adsorption, Analyst 135 (2010) 1201–1209.

[45] R. Cegielska-Radziejewska, G. Leśnierowski, J. Kijowski, Properties and application of egg white lysozyme and its modified preparations – a review, Polish J. Food Nutr. Sci. 58 (2008) 5–10.

[46] J. Sloan, Z. Liu, K. Suenaga, N.R. Wilson, P.A. Pandey, L.M. Perkins, J.P. Rourke, I.J. Shannon, Imaging the structure, symmetry, and surface-inhibited rotation of polyoxometalate ions on graphene oxide, Nano Lett. 10 (2010) 4600–4606.

[47] C. Bosch-Navarro, Z.P.L. Laker, H.R. Thomas, A.J. Marsden, J. Sloan, N.R. Wilson, J.P. Rourke, Covalently binding atomically designed Au9 clusters to chemically modified graphene, Angew. Chemie Int. Ed. 54 (2015) 9560–9563.